Eurasian Journal of Science Engineering and Technology

Research

DESIGN AND REAL-TIME IMPLEMENTATION OF EXTENDED EMF BASED POSITION-SENSORLESS DRIVE FOR SURFACE MOUNTED PERMANENT MAGNET SYNCHRONOUS MACHINES

Murat BARUT [1,*], Sung-Yoon JUNG [2], Chris MI [3]

[1,] *Department of Electrical & Electronics Engineering, Faculty of Engineering, Nigde Omer Halisdemir University, 51240, Nigde, Turkey*
[2,] *Honeywell Aerospace, Torrance, CA 90504, USA*
[3] *The U. S. Department of Energy (DOE)'s Graduate Automotive Technology Education (GATE) Center for Electric Drive Transportation, San Diego State University, San Diego, CA 92182, USA*

ABSTRACT

This paper introduces position-sensorless speed control of surface mounted permanent magnet synchronous motors (SPMSMs) based on an extended electromotive force (EMF) and specifically focuses on performances at very low and medium speeds. According to Authors' best knowledge, Morimoto's extended EMF approach is firstly applied to SPMSM and its low speed operation is evaluated by computer simulations and real-time experiments in the scope of this paper. To show that Morimoto's extended EMF technique is suitable to SPMSMs, computer simulations are executed in MATLAB® Simulink. Later, real-time experiments are performed to confirm the effectiveness of the proposed position-sensorless control system embedded on dSPACE-DS1104 controller with the SPMSM of 0.0262 Vrms/rpm. The resulting performance reveals that the possible speed estimation and thus position-sensorless control can be realized down to 1.4286% of the rated speed.

Keywords: PMSM, Position estimation, Speed estimation, Sensorless control, Extended electromotive force

1. INTRODUCTION

Nowadays permanent magnet alternating current synchronous motors (PMSMs) becomes very good option due to their reduced weight and volume causing higher power density and higher efficiency at both low and high speed operations, while the competition between different types of electrical machines is still aggressive. Considering these noticeable advantages, PMSMs get more attractive [1, 2] in variable speed drive applications consisting of hybrid electric vehicles (HEV) and electrical vehicles (EVs), industrial apparatus, renewable power generation, and home appliances in order to recover energy and space.

Further, high performance control of PMSMs calls for an accurate knowledge of rotor mechanical position and speed. However, the use of electromechanical sensors such as resolvers, optical encoders, and hall-effect sensors for this purpose increases the cost, size, weight, and hardware wiring complexity together with reducing the drive reliability and mechanical robustness [3]. Thus, position-sensorless solutions are required to discard these sensors.

In the literature, the great efforts are shown for designing position-sensorless control of PMSMs and these remarkable methods are summarized as follows [3-12]:

i) Extended EMF based methods or Back electromotive force (back-EMF).
ii) State observers utilizing deterministic or stochastic models of PMSM.
iii) The methods using high-frequency (HF) signal injection.

Mostly, the HF signal injection based methods present a stable estimation performance at very low and zero speed; however, they need to be combined with the back EMF, the extended EMF or the state observer(s) in the range of medium and high speed operations. Also, the methods without utilizing the HF signal injection are still problematic and open to research specifically at very low and zero speeds. From this point of view, it is crucial to reveal how successful and stable the estimations can be executed by the introduced methods without inclusion of the HF signal injection as the rotor speed goes down to very low and zero speeds.

Considering the position-sensorless methods mentioned above, the extended EMF technique specifically presented in Ref. [13] does not need any HF signal injection and offers very straightforward design procedure. Also, it can be easily realized in or embedded on the low-cost hardware platforms. Because Ref. [13] exploit the extended EMF estimators in order to estimate the rotor position and speed, it is very clear that the performance of this estimator is deteriorated when the rotor speed becomes very low. Because of this reason, Ref. [14] utilizes the extended EMF method in Ref. [13] together with the methods including HF signal injection. However, no effort is shown in both Ref. [13] and Ref. [14] in order to report the limit of the stable low speed

* Corresponding author, e-mail: mbarut@ohu.edu.tr;
Recieved: 14.06.2020 Accepted: 12.08.2020

estimation performance. Also, both studies [13, 14] use interior permanent magnet synchronous motors (IPMSMs) in real-time experiments to verify the proposed or implemented estimation algorithms. In addition, Ref. [13] declares that the proposed extended EMF approach is applicable to surface permanent magnet synchronous motors (SPMSMs) and the synchronous reluctance motors.

The main contribution of this paper is to implement the extended EMF based position-sensorless drive in both simulation and real time for the speed control of the SPMSM especially concentrating on very low and medium speeds. Thus, differently from the past studies [13, 14], this paper purposes

-To verify the possible limit of low speed estimation of the extended EMF method

-To validate the extended EMF method suitable to SPMSMs with the help of the challenging simulations and the real-time experiments. From this perspective, it is first known study in the literature and the extended version of the study in [15] which does not consist of the performance tests related to the simulations of the designed position-sensorless control system. The results obtained from simulation and real-time experiments proves the applicability and effectiveness of the developed position-sensorless drive system. Also, ıt is revealed that the stable low speed estimation and control can be executed till 1.4286 % of the rated speed for SPMSM with 0.0262 Vrms/rpm.

2. DEVELOPMENT OF SPEED AND POSITION ESTIMATORS BASED ON EXTENDED EMF FOR SPMSM

For this purpose, firstly the stator voltage equations [13, 14] of a PMSM in the rotating $dq-$axes can be given as:

$$v_{sd} = R_s i_{sd} + L_{sd}\frac{di_{sd}}{dt} - \omega L_{sq} i_{sq} \tag{1}$$

$$v_{sq} = R_s i_{sq} + L_{sq}\frac{di_{sq}}{dt} + \omega L_{sd} i_{sd} + \omega \psi_f \tag{2}$$

or

$$\begin{bmatrix} v_{sd} \\ v_{sq} \end{bmatrix} = \begin{bmatrix} R_s + pL_{sd} & -\omega L_{sq} \\ \omega L_{sd} & R_s + pL_{sq} \end{bmatrix} \begin{bmatrix} i_{sd} \\ i_{sq} \end{bmatrix} + \begin{bmatrix} 0 \\ \omega \psi_f \end{bmatrix} \tag{3}$$

Here, R_s is the stator resistance. L_{sd} and L_{sq} are *d* and *q* axis components of the stator inductances, respectively. i_{sd} and i_{sq} are *d* and *q* axis components of the stator inductances, respectively. ψ_f is the EMF constant. ω is the synchronous speed at which $dq-$frame rotates, as shown in Figure 1. p in (3) represents the differential operator.

Because the $dq-$model in (3) does not directly contain the rotor position, θ, it is decided to use the mathematical model represented in the estimated rotating axis named as $\gamma\delta-$frame, which lags $dq-$axes by θ_e shown in Figure 1, in Ref. [13]. Therefore, (3) is rewritten in $\gamma\delta-$frame as follows [16]:

$$\begin{bmatrix} v_\gamma \\ v_\delta \end{bmatrix} = \begin{bmatrix} R_s + pL_{sd} & -\omega L_{sq} \\ \omega L_{sq} & R_s + pL_{sd} \end{bmatrix} \begin{bmatrix} i_\gamma \\ i_\delta \end{bmatrix} + \begin{bmatrix} e_\gamma \\ e_\delta \end{bmatrix} \tag{4}$$

$$\begin{bmatrix} e_\gamma \\ e_\delta \end{bmatrix} \hat{=} E_{ex} \begin{bmatrix} -\sin\theta_e \\ \cos\theta_e \end{bmatrix} + (\hat{\omega} - \omega) L_d \begin{bmatrix} -i_\delta \\ i_\gamma \end{bmatrix} \tag{5}$$

$$E_{ex} \hat{=} \omega\left[\left(L_{sd} - L_{sq}\right) i_{sd} + \psi_f\right] - \left(L_{sd} - L_{sq}\right) p i_{sq} \tag{6}$$

Here e_γ and e_δ are named as γ and δ axis components of the extended EMF. Also, (4) is a general form applicable [13, 16] to

-SPMSM when $L_{sd} = L_{sq}$

-IPMSM when $L_{sd} < L_{sq}$

-Synchronous Reluctance Motors (SYNRMs) when $\psi_f = 0$

At this step, $\hat{e}_\gamma$ and $\hat{e}_\delta$ are firstly determined by exploiting the assumption of $L \hat{=} L_{sd} = L_{sq}$ related to SPMSM in (4) – (6) as demonstrated in Figure 2.

DESIGN AND REAL-TIME IMPLEMENTATION OF EXTENDED EMF BASED POSITION-SENSORLESS DRIVE FOR SURFACE MOUNTED PERMANENT MAGNET SYNCHRONOUS MACHINES

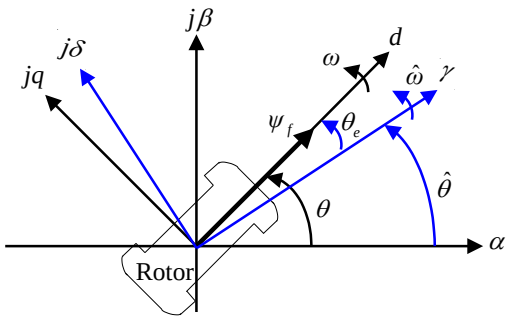

Figure 1. Positions of $\alpha\beta$ – stationary (stator-fixed) frame, dq – field frame rotating at ω, and $\gamma\delta$- estimated frame rotating at $\hat{\omega}$ for design of the extended EMF method.

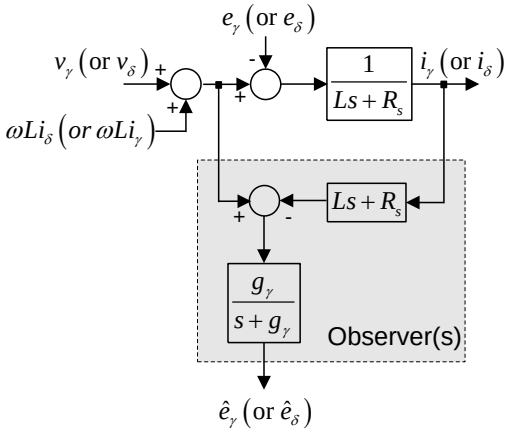

Figure 2. Least-order observer(s) for estimations of e_γ and e_δ.

Secondly, because the estimated rotor speed error, $\hat{\omega}-\omega \cong 0$, is small enough, the extended EMF can be also estimated from (5), as follows:

$$\begin{bmatrix}\hat{e}_\gamma \\ \hat{e}_\delta\end{bmatrix} = E_{ex}\begin{bmatrix}-\sin\theta_e \\ \cos\theta_e\end{bmatrix} \tag{7}$$

Finally, θ_e is estimated by

$$\hat{\theta}_e = \tan^{-1}\left(\frac{\hat{e}_\gamma}{\hat{e}_\delta}\right) \tag{8}$$

To make $\hat{\theta}_e$ equal to zero, the estimated speed ($\hat{\omega}$) and position ($\hat{\theta}$) need to be compensated by the equivalent close-loop system as shown in Figure 3. By utilizing the desired operating points related to the close-loop system, the proportional gain, K_p, and integral gain, K_i of the PI controller are obtained as:

$$K_p = 2\xi w_n,\ K_i = w_n^2 \tag{9}$$

Here, ξ and w_n are the damping ratio and the natural frequency of the desired response, respectively.

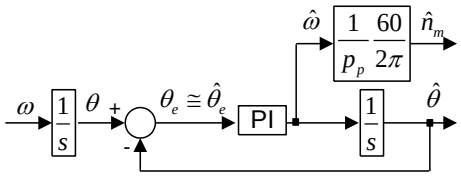

Figure 3. An equivalent close-loop system for the extended EMF based speed and position estimators

3. COMPUTER SIMULATIONS OF POSITION-SENSORLESS SPMSM DRIVE

The principle scheme of the position-sensorless SPMSM drive designed in MATLAB® Simulink is given in Figure 4. Here, the extended EMF based observer is built on Figure 3 utilizing the calculations of $\hat{e}_\gamma$ and $\hat{e}_\delta$ in Figure 2 and $\hat{\theta}_e$ in Eq. 8. In Figure 4, the speed and the current controllers are conventional PIs, and the rated parameters of the SPMSM are given in Table I. The sampling time, T, is 10μs.

Different scenarios are considered in computer simulations to show that the extended EMF based observer in this paper is applicable to SPMSMs in the design of position-sensorless drive. These scenarios focus on the performances at very low and medium speeds which are given in Figures 5 and 6. Analyzing the simulation results in Figures 5 and 6, the following observations are made:

- Transition to position-sensorless case occurs at 0.5s under *no-load* in Figure 5 and *rated-load* in Figure 6. It is observed that the transitions in both cases can be easily carried out without disturbing the desired behavior of the drive or control system.

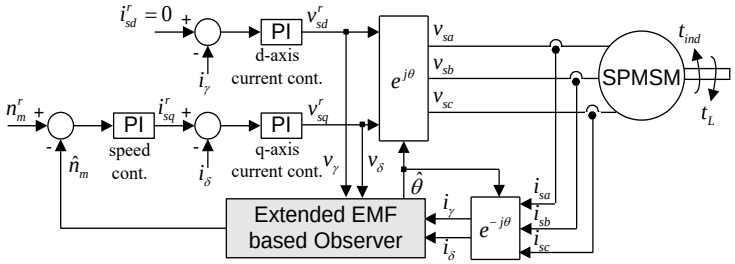

Figure 4. The principle scheme of the designed position-sensorless SPMSM drive in MATLAB® Simulink

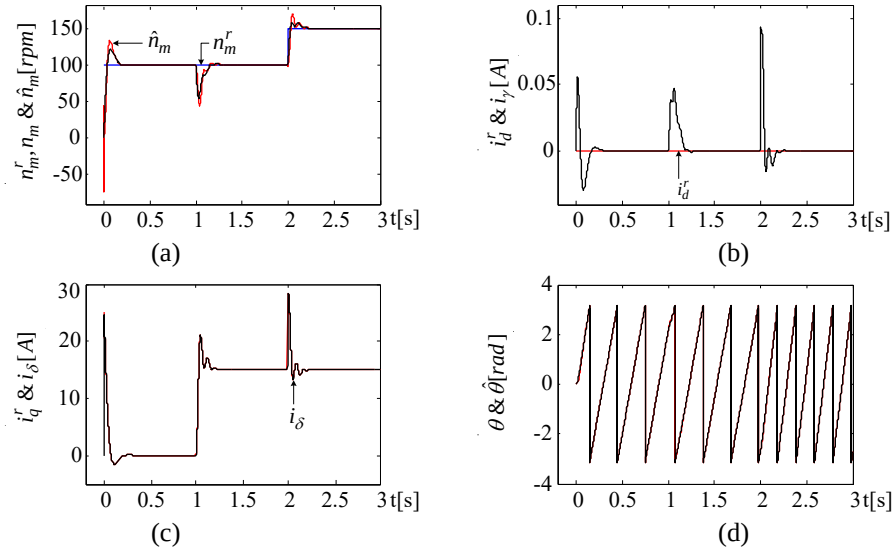

Figure 5. Simulation results at very low speeds. (a) Variations of n_m^r, n_m, and $\hat{n}_m$. (b) Variations of i_d^r and i_γ. (c) Variations of i_q^r and i_δ. (d) Variations of θ and $\hat{\theta}$.

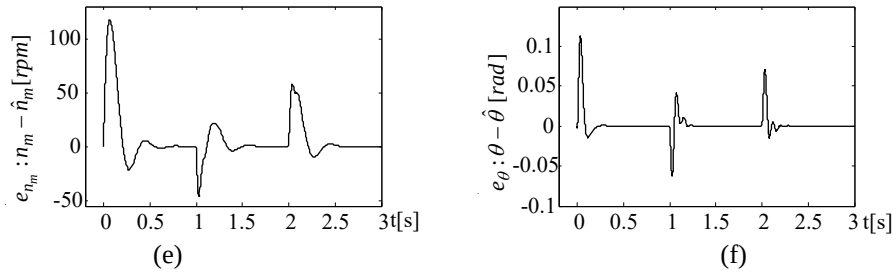

Figure 5. (Continued) Simulation results at very low speeds. (e) Variation of $e_{n_m} = n_m - \hat{n}_m$. (f) Variation of $e_\theta = \theta - \hat{\theta}$.

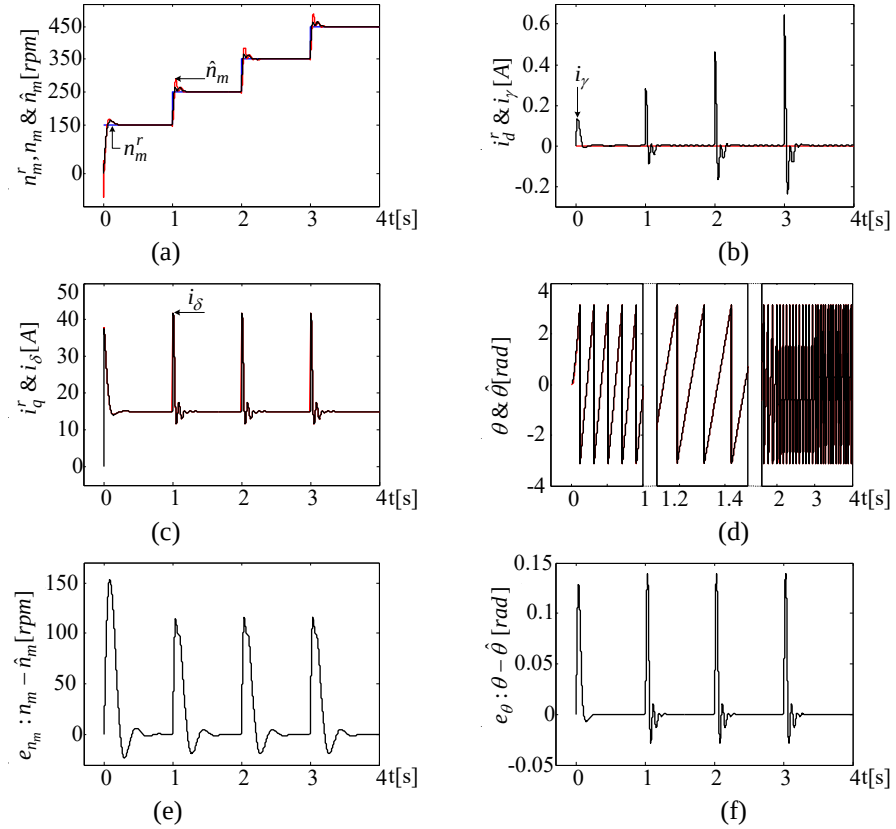

Figure 6. Simulation results at low & medium speeds. (a) Variations of n_m^r, n_m, and $\hat{n}_m$. (b) Variations of i_d^r and i_γ. (c) Variations of i_q^r and i_δ. (d) Variations of θ and $\hat{\theta}$. (e) Variation of $e_{n_m} = n_m - \hat{n}_m$. (f) Variation of $e_\theta = \theta - \hat{\theta}$.

- Under step-like changes in speed reference, n_m^r, the extended EMF based observer and thus the position-sensorless SPMSM drive demonstrate quite acceptable tracking performance at very low speeds in Figure 5 and at low and medium speeds in Figure 6.

- Inspite of the challenging variations in n_m^r in Figures 5 and 6, the estimation performances of the extended EMF based observer are very good. In addition to these variations, the load torque, t_L, is abruptly increased from 0 N.m to the rated value of 4.61 N.m at 1 s in Figure 5, the estimated states, $\hat{n}_m$ and $\hat{\theta}$, closely follow real ones, n_m and θ, respectively. These realities can be discovered by inspecting the estimation errors, $e_{n_m} = n_m - \hat{n}_m$ and $e_\theta = \theta - \hat{\theta}$, converging to zero very quickly in Figure 5(e), Figure 5(f), Figure 6(e), and Figure 6(f).

From the computer simulations, it is concluded that the extended EMF based observer in this paper is capable to work under both no-load and rated load even at very low to medium speeds; therefore, it can be used for the design of position-sensorless SPMSMs drive.

4. EXPERIMENTAL SET-UP

The general view of the real-time test bench utilized to demonstrate performances of the extended EMF based speed and position estimators and thus position-sensorless drive including SPMSM is given in Figure 7, and Table I shows rated parameters of the SPMSM. The SPMSM is loaded by separately excited direct current machine. The designed position-sensorless control system based on extended EMF is embedded in the power PC-based DS1104 controller board processing floating-point operations at a rate of 250 MHz. The incremental encoder of 2048 lines/rev is only utilized to correct position and speed estimations.

The schematic view of the implemented position-sensorless SPMSM control system is also presented in Figure 8. Here, SV-PWM denotes space vector-pulse with modulation technique. As can be seen from Figure 8, the extended EMF based estimator exploits only the stator phase currents, i_γ and i_δ, as measured variables. The required voltage signals, v_γ and v_δ, are directly achieved from the outputs of *d*- and *q*-axis current controllers.

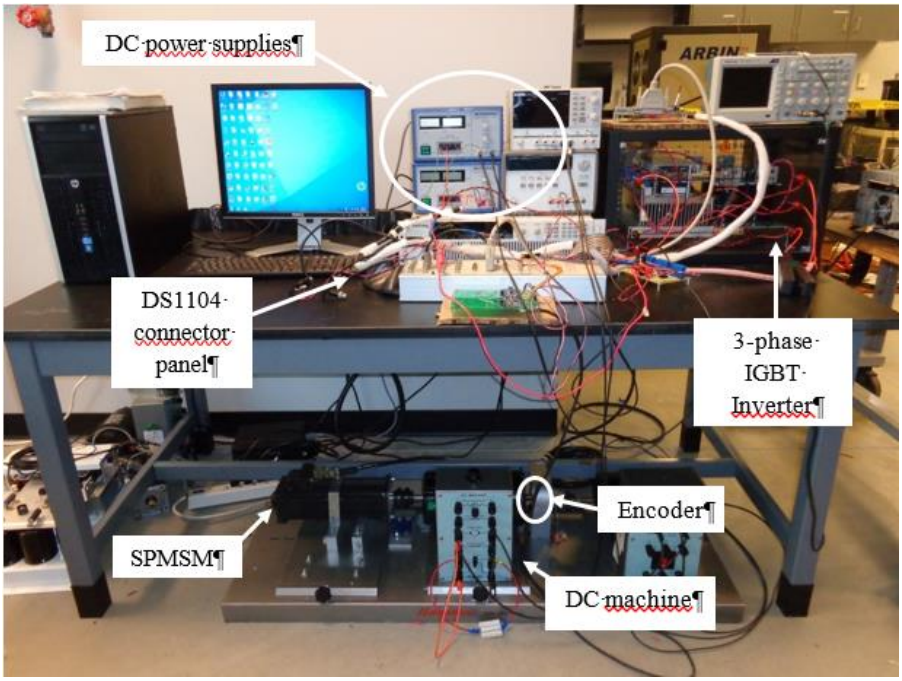

Figure 7. General view of the real-time test bench.

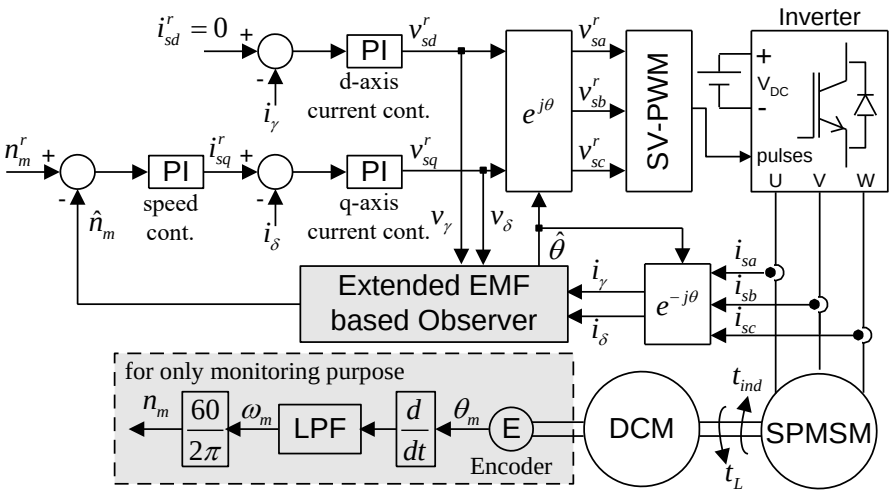

Figure 8. The principle scheme of the designed position-sensorless SPMSM drive.

5. REAL-TIME EXPERIMENTAL RESULTS

In order to evaluate the performance of the extended EMF based position-sensorless SPMSM drive in the real-time experiments with the sampling time, T, of 1/(8kHz), three scenarios are generated for the different speed operations as follows:

-Very low speed operation
-Very low and medium speed operations
-High speed operation

5.1. Performance at very low speed operation (Figure 9)

In this section, it is desired to show the lowest possible speed control limit which can be performed by the extended EMF based position-sensorless SPMSM drive. For this aim, n_m^r is instantly increased to 150 rpm at 2.7 s and decreased to 100 rpm at 7.5 s speed while the SPMSM rotates at 100 rpm. The resulting performance is presented in Figure 9. As demonstrated in Figure 9(a) and (e), $\hat{n}_m$ closely tracks n_m. The speed and current controllers also show satisfactory tracking performance in Figure 9(a), (b), and (c). Moreover, inspecting Figure 9(d) and (f), it can be seen that the average value of $e_\theta = \theta - \hat{\theta}$ is about 0.6480[rad] (37.12 Deg). As n_m^r (or n_m) approaches to zero, $e_\theta = \theta - \hat{\theta}$ gets increased since the extended EMF term is deteriorated with the increasing noise on the measured i_γ and i_δ and finally vanishes. For the SPMSM with 0.0262 Vrms/rpm, it is observed that the acceptable position-sensorless close-loop speed control can be performed down to 100 [rpm] which is equal to 1.4286 % of the rated speed.

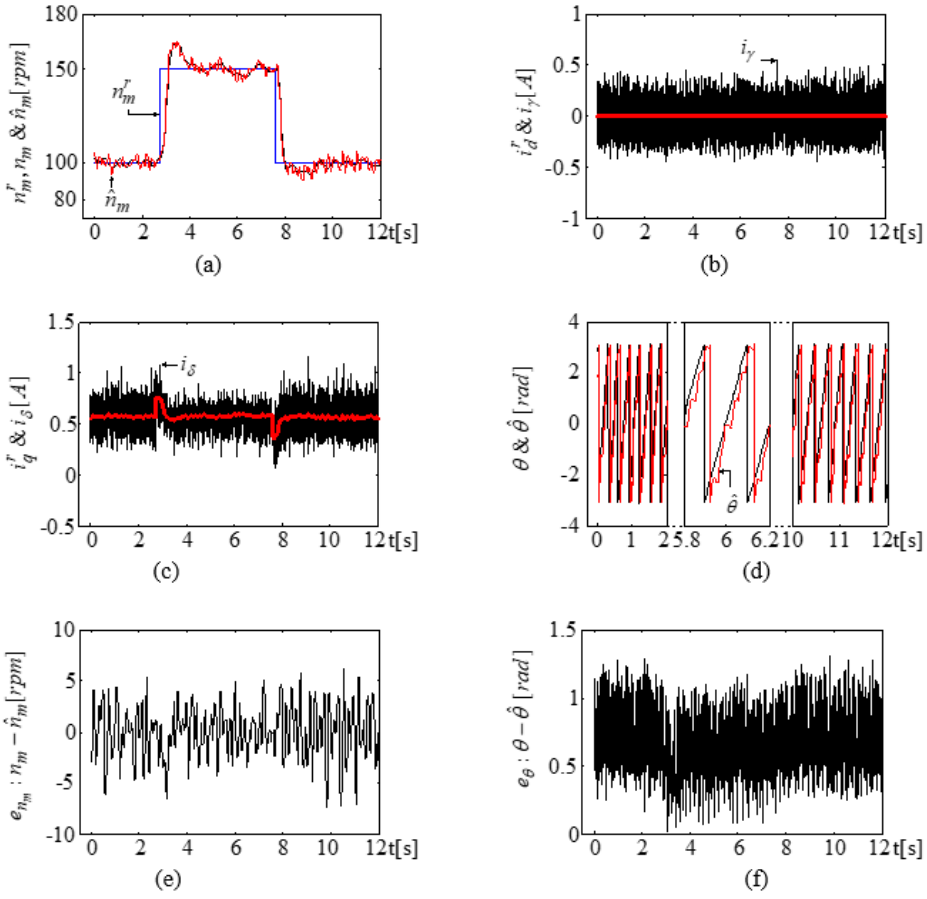

Figure 9. Real-time results at very low speeds. (a) Variations of n_m^r, n_m, and $\hat{n}_m$. (b) Variations of i_d^r and i_γ. (c) Variations of i_q^r and i_δ. (d) Variations of θ and $\hat{\theta}$. (e) Variation of $e_{n_m} = n_m - \hat{n}_m$. (f) Variation of $e_\theta = \theta - \hat{\theta}$.

5.2. Performance at very low and medium speed operations (Figure 10)

This scenario aims to illustrate the transition performance of the position-sensorless drive from the very low speeds to medium speeds. Therefore, the increased step-like variations of 150 [rpm] are given to n_m^r from [150] rpm to 600 [rpm], and the obtained results are given in Figure 10. Figures 10(a), (b), and (c) validate the successful control performances of the speed and current controllers while Figures 10(d) and (e) verify the very good estimation performances of the speed and position. Further, as can be seen from Figure 10(d) and (e), after the step change in n_m^r at 2 s, $e_\theta = \theta - \hat{\theta}$ suddenly decreases to very small values. Namely, $e_\theta = \theta - \hat{\theta}$ becomes smaller when n_m^r (or n_m) raises, as expected.

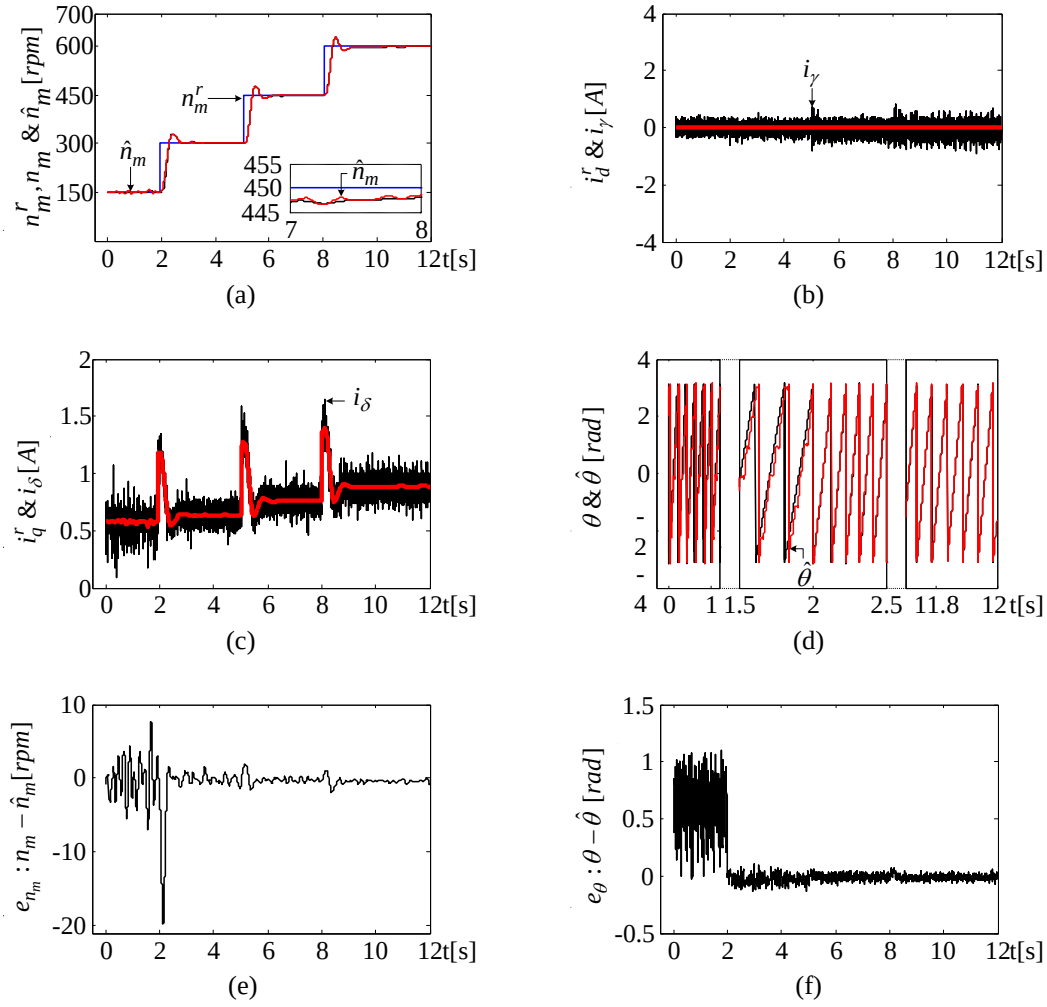

Figure 10. Real-time results at low & medium speeds. (a) Variations of n_m^r, n_m, and $\hat{n}_m$. (b) Variations of i_d^r and i_γ. (c) Variations of i_q^r and i_δ. (d) Variations of θ and $\hat{\theta}$. (e) Variation of $e_{n_m} = n_m - \hat{n}_m$. (f) Variation of $e_\theta = \theta - \hat{\theta}$.

5.3. Performance at high speed operation (Figure 11)

In this scenario, it is also aimed to show the high speed control and estimation performances of the developed position sensorless SPMSM drive. For this pupose, n_m^r is stepped down to 1250 [rpm] at 1.8 s, 1100 [rpm] at 4.9 s, and 950 [rpm] at 7.9 s, respectively while the SPMSM revolves at 1400 [rpm]. The results given in Figure 11 for this scenario confirm the perfect tracking and estimation abilities of the designed extended EMF based position-sensorless SPMSM drive.

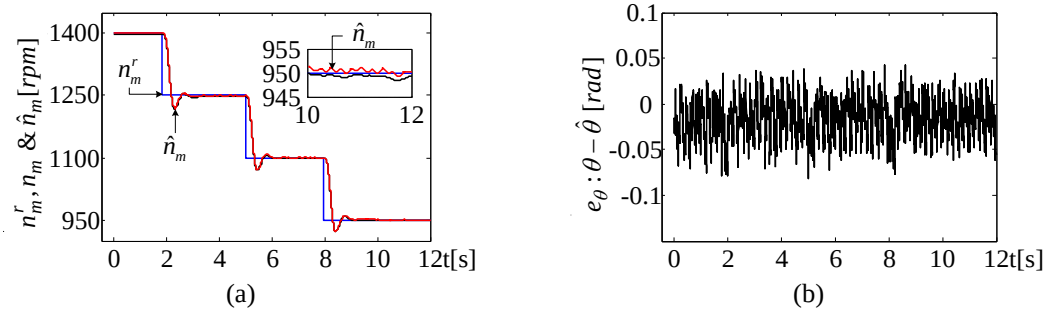

Figure 11. Real-time results at high speeds. (a) Variations of n_m^r, n_m, and $\hat{n}_m$. (f) Variation of $e_\theta = \theta - \hat{\theta}$.

6. CONCLUSION

In this paper, an extended EMF based position-sensorless control system has been developed for the speed control of SPMSM and realized in simulations and real-time experiments in order to reveal that the extended EMF method proposed in Ref. [13] including IPMSM is also suitable to SPMSMs. For this purpose, the computer simulations are firstly executed to demonstrate that the extended EMF based observer is capable to serve for the design of the position-sensorless SPMSM drive. Later, the real-time experiments are performed to show achievements of the extended EMF based position-sensorless drive at very low, medium, and high speeds. Both the computer simulations and real-time experimental results have validated the feasibility and effectiveness of the proposed position-sensorless drive in this paper. Moreover, differently from Refs. [13] and [14], this study has specifically concentrated on the performance at very low speeds. As a result, the low speed operation by the developed position-sensorless close-loop speed control system including the EMF approach in Ref. [13] is possible till 100 rpm (1.4286 % of the rated speed) for the SPMSM with 0.0262 Vrms/rpm. These efforts are firstly introduced to the current literature in the scope of this paper.

ACKNOWLEDGEMENT

The authors gratefully acknowledge the financial support from Chrysler and US DOE Grant DEEE0002720 and DE-EE0005565, and Post Doct-Grant 2219-International Post Doctoral Research Fellowship Programme by the Scientific and Technological Research Council of Turkey (TUBITAK)

APPENDIX

The rated parameters of the SPMSM are given in Table I.

Table 1. Rated parameters of the SPMSM used in real-time experiments

Parameter	Symbol	Value	Unit	Parameter	Symbol	Value	Unit
Pole pair	p_p	2	-	Rated speed	n_m	7000	Rpm
Rotor pole flux	ψ_f	0.10214	V.s	Rated torque	t_L	4.61	Nm
d-inductance	L_{sd}	0.01	H	Rated phase current	I_s	15	Arms
q-inductance	L_{sq}	0.01	H	Rated L-L Voltage	V_s	230	Vrms
Stator resistance	R_s	0.19	Ω	Rated power	P	4.5	kW

REFERENCES

[1] K. T. Chau, C. C. Chan, and C. Liu, "Overview of permanent-magnet brushless drives for electric and hybrid electric vehicles," *IEEE Transaction on Industrial Electronics*. vol. 55, no. 6, pp. 2246-2257, 2008.

[2] R. Bojoi, M. Pastorelli, J. Bottomley, P. Giangrande, and C. Gerada, "Sensorless control of PM motor drives — A technology status review," 2013 IEEE Workshop on Electrical Machines Design Control and Diagnosis (WEMDCD) Paris, France, 2013, pp. 168-182.

[3] Y. Zhao, W. Qiao, and L. Wu, "An Adaptive Quasi Sliding-Mode Rotor Position Observer-Based Sensorless Control for Interior Permanent Magnet Synchronous Machines," *IEEE Transactions on Power Electronics*, vol. 28, no.12, pp. 5618-5629, 2013.

[4] G.Wang, M. Valla, and J. Solsona, "Position Sensorless Permanent Magnet Synchronous Machine Drives—A Review," *IEEE Transaction on Industrial Electronics*. vol. 67, no. 7, pp. 5830-5842, 2020.

[5] C. Gong, Y. Hu, J. Gao, Y. Wang, and L. Yan, "An Improved Delay-Suppressed Sliding-Mode Observer for Sensorless Vector-Controlled PMSM," *IEEE Transaction on Industrial Electronics*. vol. 67, no. 7, pp. 5913-5923, 2020.

[6] C. Lascu and G.-D.Andreescu, "PLL Position and Speed Observer With Integrated Current Observer for Sensorless PMSM Drives," *IEEE Transaction on Industrial Electronics*. vol. 67, no. 7, pp. 5990-5999, 2020.

[7] C. M. Verrelli, S. Bifaretti, E. Carfagna, A. Lidozzi, L. Solero, F. Crescimbini, and M. D. Benedetto, "Speed Sensor Fault Tolerant PMSM Machines: From Position-Sensorless to Sensorless Control," *IEEE Transactions on Industry Applications*, vol. 55, no. 4, pp. 3946-3954, 2019.

[8] M. Boussak, "Implementation and experimental investigation of sensorless speed control with initial rotor position estimation for interior permanent magnet synchronous motor drive," *Transactions on Power Electronics*, vol. 20, no. 6, pp. 1413-1422, 2005.

[9] O. Benjak and D. Gerling, "Review of position estimation methods for IPMSM drives without a position sensor part I: Nonadaptive methods," 2010 XIX Int. Conf. on Electrical Machines (ICEM) Rome, Italy, 2010, on CD.

[10] O. Benjak and D. Gerling, "Review of position estimation methods for IPMSM drives without a position sensor part II: Adaptive methods", 2010 XIX Int. Conf. on Electrical Machines (ICEM) Rome, Italy, 2010, on CD.

[11] A. Sarikhani and O.A. Mohammed, "Sensorless control of PM synchronous machines by physics-based EMF observer," *IEEE Transaction on Energy Conversion*. vol. 27 no. 4, pp. 1009-1017, 2012.

[12] Y. Zhao, Z. Zhang; W. Qiao, and L. Wu, "An extended flux model-based rotor position estimator for sensorless control of salient-pole permanent-magnet synchronous machines," *IEEE Transactions on Power Electronics*, vol. 30, no.8, pp. 4412-4422, 2015.

[13] S. Morimoto, K. Kawamoto, M. Sanada, and Y. Takeda, "Sensorless control strategy for salient-pole PMSM based on extended EMF in rotating reference frame," *IEEE Transactions on Industry Applications*, vol. 38, no. 4, pp. 1054-1061, 2002.

[14] J. Hong, S. -Y, Jung, and K. Nam, "An incorporation method of sensorless algorithms: Signal injection and back EMF based methods," 2010 Int. Power Electron. Conf. (IPEC) Sapporo, Japan, 2010, pp. 2743-2747.

[15] M. Barut, S.-Y. Jung, and C. Mi, "Real-time performance evaluation of extended EMF based sensorless drive for SPMSMs," 2014 XXIth Int. Conf. on Electrical Machines (ICEM) Berlin, Germany, 2014, pp. 884-889.

[16] Z. Chen, M. Tomita, S. Ichikawa, S. Doki, and S. Okuma, "Sensorless control of interior permanent magnet synchronous motor by estimation of an extended electromotive force,"2000 IEEE- Ind. App. Conf., Rome, Italy, 2000, pp. 1814-1819.